Title:

Energy extraction from the biologic battery in the inner ear

Authors:

Patrick P. Mercier[1,2]*,Andrew C. Lysaght[3,4]*, Saurav Bandyopadhyay[1]*, Anantha P. Chandrakasan[1]+, Konstantina M. Stankovic[3,4,5]+

[1]Microsystem Technology Laboratories, Massachusetts Institute of Technology, Cambridge, Massachusetts, USA.
[2]Present address: Department of Electrical and Computer Engineering, University of California, San Diego, La Jolla, California, USA
[3]Eaton Peabody Laboratory and Department of Otolaryngology, Massachusetts Eye and Ear Infirmary, Boston, Massachusetts, USA.
[4]Program in Speech and Hearing Bioscience and Technology, Harvard / Massachusetts Institute of Technology Joint Division of Health Sciences and Technology, Cambridge, Massachusetts, USA.
[5]Department of Otology and Laryngology, Harvard Medical School, Boston, Massachusetts, USA.

* these authors have contributed equally
+ these authors have contributed equally

Correspondence should be addressed to A.P.C. (anantha@mtl.mit.edu) or K.M.S. (Konstantina_Stankovich@meei.harvard.edu)

Introduction paragraph:

The endocochlear potential (EP) is a battery-like electrochemical gradient found in and actively maintained by the inner ear[1,2]. The EP has never before been used as a power source for electronic devices. Here we demonstrate, for the first time, that it is possible to operate an electronic system using a mammalian EP as the source of energy into the system. This was achieved by designing an anatomically-sized, ultra-low quiescent-power energy harvester integrated with a wireless sensor. Although other forms of *in-vivo* or electrochemical energy harvesting have been previously shown[3-8], none are currently suitable to power implanted electronic devices in the vicinity of the ear, eye, and brain of mammals. With future research in electrode design, we envision using this biologic

battery to power chemical sensors or drug-delivery actuators, enabling transformative opportunities for new diagnostics and therapies in hearing research and related fields.

Main Text:

Implantable electronics for medical applications typically require large energy reservoirs to operate reliably over long periods of time. In both human healthcare and animal studies, anatomy often limits the size of implantable batteries, requiring surgical re-implantation or cumbersome external wireless power sources for long-term operation. Harvesting energy from nearby energy sources is an alternative approach to extend implant life, and with sufficient available energy, to allow the implant to operate autonomously. Since humans and animals already generate and consume a vast amount of power[9], biologically-based energy harvesting is a potentially well suited solution to power implanted devices. However, some biologically-derived energy sources such as heat differentials[3] and muscle movements[10] are not suitable for mammalian implantable applications due to the requirements of externally worn apparatuses. While promising, previously described *in-vivo* energy sources, such as kinetic vibrations[4] and biofuel cells[5-8,11], are inherently intermittent, are not generated by mammals, or are presently too difficult to extract in anatomically-sized devices.

At 70–100 mV, the EP is the largest positive direct current (DC) electrochemical potential in mammals, and is the main driving force for cochlear mechanotransduction of sound pressure vibrations to neurotransmitter release and excitation of the auditory nerve. Although the EP is well understood and modeled[2,12,13], it has never before been harvested

to drive electronics. Its inherent stability over mammalian lifetime[14] makes it a potential candidate for powering long-term energy-autonomous implantable devices. The EP is found within endolymph – a specialized inner ear fluid with a uniquely higher concentration of potassium than is found intracellularly. Endolymph is separated from the surrounding extracellular spaces bathed in perilymph, which is similar in ionic composition to the cerebrospinal fluid, by a complex network of tight junctions (Fig. 1). The EP effectively acts as a biologic battery whose potential is actively stabilized by a specialized arrangement of potassium channels, pumps and cotransporters (Fig. 2) in cells of the stria vascularis, a specialized structure that borders the endolymphatic space.

Any electronic system that interfaces and extracts power from the EP should not interfere with normal function of the cochlea. Total current flow through the guinea pig cochlea (including both sensory and non-sensory cells), whose anatomy and physiology is similar to that of humans, has been previously determined to be 0.8-1.6 μA/mm of cochlear wedge[15]. Given the 18 mm length of the guinea pig cochlea[16], currents generated by the stria vascularis on the order of 14-28 μA occur in the guinea pig physiologically, and place an upper limit on extractable electric current from the cochlea.

In practice, the maximum current extractable from the EP by an implanted energy harvester is constrained well below this limit by high impedance electrodes, which are designed to have sharp tips such that, when inserted into the EP space, collateral cell damage is minimized. The input power to the implantable energy harvester, which we refer to as the endoelectronics chip, is given as:

$$P = V_{IN}^2/R_{in,eff} = [V_{EP}/(R_{in,eff}+R_{elec})]^2.R_{in,eff}$$

where V_{EP} is the endocochlear potential, R_{elec} and $R_{in,eff}$ are the impedances of the glass electrodes and the endoelectronics chip, respectively, and V_{IN} ($=V_{EP}R_{in,eff}/(R_{in,eff}+R_{elec})$) is the effective input voltage to the endoelectronics (Fig. 2). To maximize the extractable power given electrode impedance constraints, $R_{in,eff}$ needs to be configured close to R_{elec}. For traditionally used glass microelectrodes, the tradeoff between electrode impedance and bluntness reaches a point of diminishing returns at R_{elec} = 0.4–1.1 MΩ. This results in extractable power ranging from 1.1–6.3 nW with V_{IN} in the range of 30–55 mV.

The low EP voltage, in conjunction with low extractable power, poses two significant challenges for harvesting net positive energy. First, transistor-based electronics require hundreds of millivolts to start-up without requiring expensive semiconductor post processing[17,18]. Second, the maximum extractable power levels are at least an order of magnitude less than the quiescent power of the most efficient energy harvesting and sensing circuits in the literature[19-21]. For continuous, self-sustaining operation, quiescent power should be well below the maximal extractable power.

We overcame the challenges of energy harvesting from the EP with a custom integrated circuit featuring a wireless kick-start energy receiver and ultra-low-quiescent-current energy-buffering power electronics. The low-voltage turn-on issue was addressed by delivering an initial one-time wireless start-up charging packet of less than two seconds between an external radio frequency (RF) source and an on-board 3x4 mm^2 loop antenna. This charging packet was converted from RF power to DC in order to charge a 200 nF energy buffer capacitor, C_{DD} (Fig. 2), up to a maximum of 1.4 V. At such a voltage, C_{DD} contained up to 200 nJ, which was sufficient to operate the system for at most six minutes before the stored energy was completely exhausted (given a total system power

consumption of 573 pW as discussed below). To sustain the charge on C_{DD} once the external RF source was removed, a boost converter harvested the low-voltage EP energy by transferring and converting this energy to a higher voltage suitable for buffering energy onto C_{DD}. For system sustainability, the quiescent power consumption of the circuits that control the boost converter should be much less than the available output power. We implemented a continuously running timer and driver circuits that consumed 527 pW at 0.9 V, controlling the boost converter and activating a load circuit every 40-360 seconds. The boost converter achieved an efficiency of 53.4%. After including the timer and driver overhead, 60–2840 pW of net positive power was extracted and available for the load circuit.

In any implanted sensing system, communication is essential to convey sensed information to the external world. Here, we integrated a wireless radio transmitter that, through the use of extensive leakage power reduction techniques[22], consumed a standby power of 46 pW at 0.9 V. To minimize the implant's physical volume, the transmitter shared the on-board antenna with the wireless kick-start circuit. The output data rate was set by an integrated ring oscillator, and could operate at instantaneous data rates programmable from 100 kbps to 10 Mbps up to a 1 m distance. Combined, the active energy consumption, packet length, and standby power dictate the maximum frequency of packet transmissions. With the given power budget, the transmitter spent approximately 0.0001% of its time in active mode.

The chip was fabricated in a standard complementary metal-oxide-semiconductor (CMOS) process with a minimum feature size of 0.18 μm, and occupied a total volume of 2.4x2.4x0.2 mm^3. The chip was wirebonded to a printed circuit board prototype (Fig. 3a)

that is currently sufficiently small to be implantable in the human mastoid cavity, or in the bulla cavity of cats, gerbils, or chinchillas (Fig. 1)[23].

We operated the chip for up to five hours using the EP of an anesthetized Hartley Albino *Cavia porcellus* (guinea pig) as the source of energy into the system, following an initial wireless kick-start. For feasibility studies, the system was operated externally, with the electrode tips inserted into the cochlea and the electrode shafts connected to the endoelectronics chip located externally (Supplementary Fig. 1). Figure 3b shows the C_{DD} system supply voltage, V_{DD}, which replenished and persisted throughout a 20 minute measurement (Supplementary Fig. 2 shows the results from a five hour experiment). Since the system operated longer than the energy contained in the initial kick-start otherwise permitted, these results demonstrate, for the first time, an energy harvesting system powered primarily from a mammalian electrochemical potential As the boost converter's average input impedance was configured to approximately equal the electrode impedance, the converter extracted close to the maximal possible power from the EP given physical constraints of electrodes. As a result, V_{DD} slowly fluctuated as the animal's EP, and therefore the available energy into the system varied. On a smaller time scale, as shown in Fig. 3c for three different experiments, V_{DD} periodically dropped by 36–48 mV during active-mode wireless transmissions. Following the voltage drop, the boost converter continued to harvest energy from the EP by trickle-charging capacitor C_{DD}, thereby recovering energy spent during the transmission.

We used energy harvested from the EP to not only power a wireless transmitter, but also to sense relative changes in the EP after the voltage drop seen in the electrode resistance (i.e., V_{IN}). Because the instantaneous radio data rate was generated internally by a ring

oscillator whose frequency varied with V_{DD} (which in turn varied with the EP and therefore V_{IN}), the wirelessly received data bits were inherently encoded with EP information. Thus, by monitoring the output data rate we demonstrated a self-powered system that is also capable of continuously monitoring relative changes in the EP (Fig. 3d). Trends in sensed V_{IN} ($=V_{EP}.R_{in,eff}/(R_{in,eff}+R_{elec})$), powered by the EP, were within a 0.45 mV RMS error of direct measurements by an external battery-powered device over a 2.5 hour experiment.

To test whether the system affected hearing, compound action potential thresholds were measured before and after electrode insertion (Supplementary Fig. 3), and before and after current draw (Fig. 3e) in two different anesthetized guinea pigs, respectively. Because the cochlea is tonotopically organized, with the high frequencies encoded at the cochlear base, and low frequencies encoded at the cochlear apex, cochlear function was tested along its length by using tone pips of different frequencies. Insertion of the beveled glass microelectrodes did not adversely affect hearing (Supplementary Fig. 3). Likewise, current draw during the experiment shown in Fig. 3b had essentially no effect on hearing for frequencies up to 16 kHz (Fig. 3e). A small degradation in threshold was observed at a frequency of 23 kHz, which is encoded close to the round window (near the cochlear base). This degradation is likely due to the electrode tip, which was designed to be ~2 μm in diameter after beveling so to allow low electrode impedance, typically ~ 800 kΩ, which is required for energy extraction from the EP. At such sizes, electrodes can cause local physical trauma to the cells lining the basilar membrane, and thereby allow leakage of ions across the endolymph-perilymph barrier, as well as leakage of ions from the fluid-filled electrodes into cochlear fluids. In contrast, electrodes that have been used to stably

record the EP for many hours have tips < 1 μm in diameter, and impedances greater than 5 megaohms[24]. Taken together, our data point that major improvements in electrode design are required to allow eventual long-term energy extraction from the EP. In the meantime, our prototype system demonstrates feasibility with minimal effect on hearing in a short run.

With future miniaturization of low-impedance electrode tip, and with refinements in minimally invasive surgical approaches to endolymph, (e.g. via Reissner's membrane[25]), our system would be useful in animal studies with far-reaching implications for biotechnology and medicine. For example, since small rodents are commonly used in hearing research, the proposed energy harvesting system could enable miniaturized and fully implantable sensing systems with minimal risk of malfunction from external infections or trauma. We envision implementing chemical and other electronic sensors and actuators, not only in the cochlea and the nearby vestibular end organs of the inner ear (Fig. 1), but also in the adjacent structures such as the temporal lobe of the brain, facial nerve, and carotid artery, all of which are within millimeters of the cochlea.

In the future, energy extraction from the cochlea may be applicable to humans. Surgical insertion of devices, such as cochlear implants and stapes prostheses, into the human inner ear is already possible with minimal risks of damaging normal or residual hearing[26,27]. Although the risk of hearing loss is higher when inserting an electrode into endolymph than perilymph, there are many forms of deafness where the EP is normal, such as deafness due to loss of sensory cells, cochlear neurons, or supporting cells. In such cases, the benefit of a battery-less system for sensing of key molecules in the inner ear may outweigh the potential risk to the EP during electrode insertion into endolymph.

Although we have identified and overcome key challenges in developing the components of the system necessary to harvest net positive energy from the inner-ear for hours at a time, important future work is required in electrode miniaturization and surgical approaches in order to advance from demonstrating feasibility, to integrating all components into a safe, fully-implantable system for long-term operation.

References:

1. Von Bekesy, G. Resting potentials inside the cochlear partition of the guinea pig. *Nature* **169**, 241–242 (1952)
2. Hibino, H., Nin, F, Tsuzuki, C. & Kurachi, Y. How is the highly positive endocochlear potential formed? The specific architecture of the stria vascularis and the roles of the ion-transport apparatus. *Pflügers Archiv European Journal of Physiology* **459**, 521-533 (2010)
3. Hochbaum, A. I. *et al.* Enhanced thermoelectric performance of rough silicon nanowires. *Nature* **451**, 163–167 (2008)
4. Qin, Y., Wang, X. & Wang, Z. L. Microfibre–nanowire hybrid structure for energy scavenging. *Nature* **451**, 809-813 (2008)
5. Chaudhuri, S. K. & Lovley, D. R. Electricity generation by direct oxidation of glucose in mediatorless microbial fuel cells. *Nature Biotechnology* **21**, 1229-1232 (2003)
6. Himes, C., Carlson, E., Ricchiuti, R. J., Otis, B. P., & Parviz, B. A. Ultralow Voltage Nanoelectronics Powered Directly, and Solely, From a Tree. *IEEE Trans. Nanotechnology* **9**, 2-5 (2010)
7. Rasmussen, M., Ritzmann, R. E., Lee, I., Pollack, A. J., & Scherson, D. An Implantable Biofuel Cell for a Live Insect. *J. Am. Chem. Soc.* **134**, 1458-1460 (2012)
8. Halámková, L. *et al.*Implanted Biofuel Cell Operating in a Living Snail. *J. Am. Chem. Soc.* **134**, 5040-5043 (2012)
9. Starner, T. & Paradiso, J.A. Human-generated power for mobile electronics. *Low Power Electronics Design*, CRC Press, Chapter 4, 1-35 (2004)
10. Donelan, J. M. *et al*. Biomechanical energy harvesting: generating electricity during walking with minimal user effort. *Science* **319**, 807-810 (2008)
11. Bullen, R. A., Arnot, T. C., Lakeman, J. B., & Walsh, F. C. Biofuel cells and their development. *Biosensors and Bioelectronics* **21**, 2015-2045 (2006)
12. Dallos, P. Some electrical circuit properties of the organ of Corti. I. Analysis without reactive elements. *Hearing Research* **12**, 89-119 (1983)
13. Takeuchi, S. and Ando, M., & Kakigi, A. Mechanism generating endocochlear potential: role played by intermediate cells in stria vascularis. *Biophysical J.* **79**, 2572-2582 (2000)
14. Lang, H., Schulte, B.A., & Schmiedt, R.A. Endocochlear potentials and compound action potential recovery: functions in the C57BL/6J mouse. *Hearing Research* **172**, 118-126 (2002)

15. Zidanic, M. & Brownell, W.E. Fine structure of the intracochlear potential field. I. The silent current. *Biophysical J.* **57**, 1253-1268 (1990)
16. Fernandez, C. Dimensions of the cochlea (guinea pig). *J. Acoust. Soc. Am.* **24**, 519-523 (1952)
17. Swanson, R.M. & Meindl, J.D. Ion-implanted complementary MOS transistors in low-voltage circuits. *IEEE ISSCC Dig. Tech. Papers*, 192–193 (1972)
18. Chen, P.-H. *et al.*A 95mV-startup step-up converter with V_{TH}-tuned oscillator by fixed-charge programming and capacitor pass-on scheme. *IEEE ISSCC Dig. Tech. Papers*, 216-217 (2011)
19. Ramadass, Y.K. & Chandrakasan, A.P., A battery-less thermoelectric energy harvesting interface circuit with 35mV startup voltage. *IEEE J. Solid-State Circuits* **46**, 333-341 (2011)
20. Shimamura, T. *et al.* Nano-watt power management and vibration sensing on a dust-size batteryless sensor node for ambient intelligence applications. *IEEE ISSCC Dig. Tech. Papers*, 540-541 (2010)
21. Wieckowski, M., Chen, G.K., Seok, M., Blaauw, D. & D. Sylvester, D. A hybrid DC-DC converter for sub-microwatt sub-1V implantable applications. *IEEE Symposium on VLSI Circuits*, 166-167 (2009)
22. Roy, K., Mukhopadhyay, S., & Mahmoodi-Meimand, H., Leakage current mechanisms and leakage reduction techniques in deep-submicrometer CMOS circuits. *Proceedings of the IEEE* **91**, 305-327 (2003)
23. Mason, M.J. Middle ear structures in fossorial mammals: comparison with non-fossorial species. *J. Zool. Lond* **255**, 467-486 (2001)
24. Mills, D.M., Norton, S.J., & Rubel, E.W. Vulnerability and adaptation of distortion product otoacoustic emissions to endocochlear potential variation. *J. Acoust. Soc. Am.* **94**, 2108-2122 (1993)
25. Von Bekesy, G. DC resting potentials inside the cochlear partition. *J. Acoust. Soc. Am.* **24**, 72 (1952)
26. Fayad, J.N., Semaan, M.T., Meier, J.C., House JW. Hearing results using the Smart piston prosthesis. *Otol Neurotol* **30,** 1122-7 (2009)
27. Mowry, S.E., Woodson, E., Gantz, B.J. New frontiers in cochlear implantation: acoustic plus electric hearing, hearing preservation, and more. *Otolaryngol Clin North Am* **45,** 187-203 (2012)

Acknowledgements:

The authors acknowledge the support of the C2S2 Focus Center and the Interconnect Focus Center, two of six research centers funded under the Focus Center Research Program (FCRP), a Semiconductor Research Corporation entity (A.P.C., P.P.M., S.B.), NIH grants K08 DC010419 (K.M.S.) and T32 DC00038 (A.C.L.), and the Bertarelli Foundation (K.M.S.). We thank Dr. John J. Guinan Jr. for experimental assistance and advice, and Bo Zhu for preliminary studies.

Author Contributions:

A.P.C. and K.M.S. conceived the project. P.P.M., A.C.L., S.B., A.P.C. and K.M.S. designed experiments. P.P.M., A.C.L. and S.B. performed the experiments. P.P.M. and S.B. designed and implemented the electronic chip. A.C.L. performed the EP measurements. P.P.M., A.C.L., S.B., A.P.C. and K.M.S. wrote and edited the manuscript.

Author Information:

The authors declare no competing financial interests. Correspondence and requests for materials should be addressed to K. M. S. (konstantina_stankovic@meei.harvard.edu) or A.P.C. (anantha@mtl.mit.edu).

Figure legends:

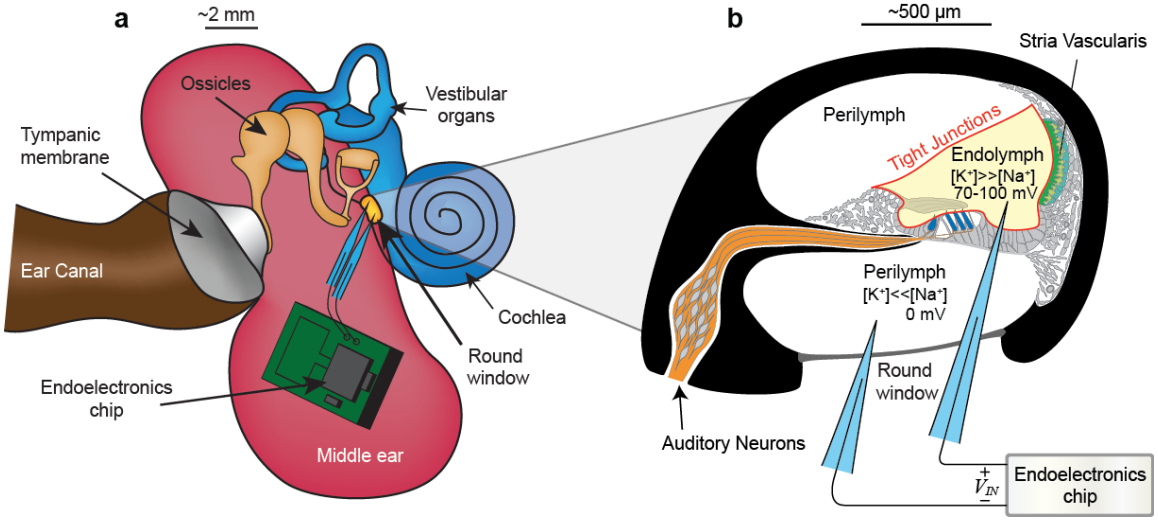

Figure 1 | Anatomy and physiology of the inner ear. **a.** Schematic of a mammalian ear including the external, middle, and inner ear, which includes the cochlea and vestibular end organs. **b.** Cross section of a typical cochlear half turn highlighting the

endolymphatic space (yellow) bordered by tight junctions (red), the stria vascularis (green) and hair cells (blue), which are contacted by primary auditory neurons (orange).

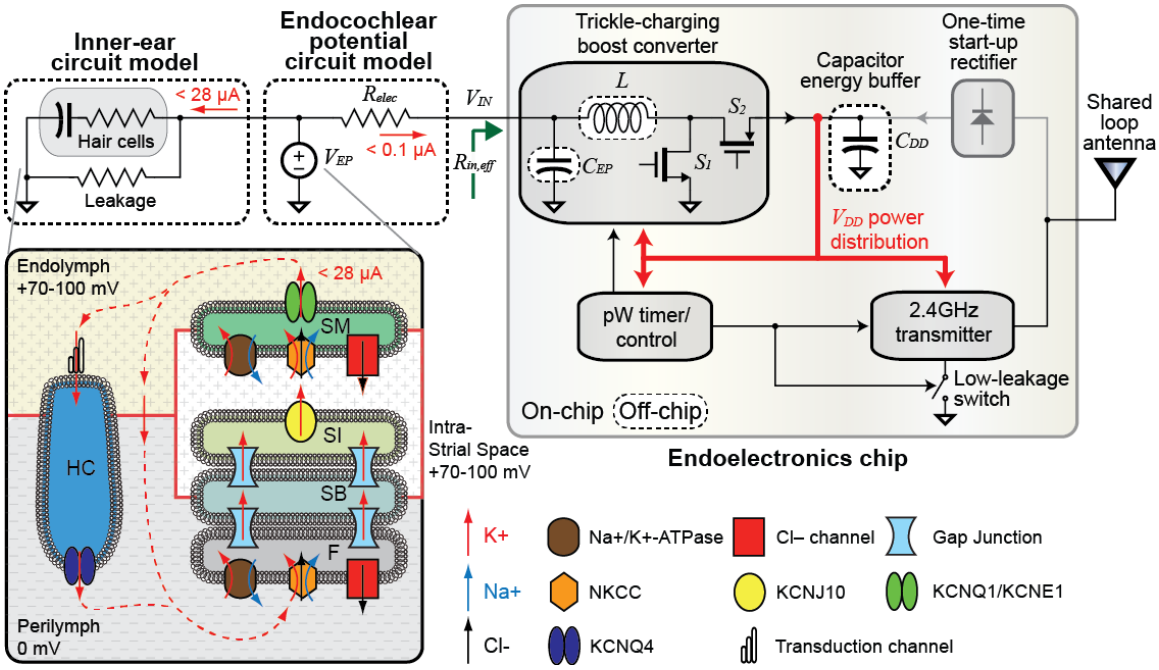

Figure 2 | Schematic of the endoelectronics chip and equivalent circuit model of the endocochlear potential and inner ear tissues. To generate and maintain EP, perilymphatic K^+ enters fibrocytes (F) via Na^+/K^+-ATPase and Na-K-Clcotransporter. Gap junction networks connect F to strial basal (SB) and intermediate (SI) cells, allowing ions to enter the intra-strial space via KCNJ10 channels. Strial marginal (SM) cells uptake K^+ against a significant concentration gradient and release K^+ into endolymph. K^+ returns to perilymph either by entering hair cells (HC) apically during mechano-electrical transduction of sound and exiting basolaterally via KCNQ4 channels, or via leakage current through the surrounding tissues (solid red lines represent tight-junction networks). With energy from the EP, a boost converter was used to trickle-charge capacitor C_{DD}, which supplies power to an integrated wireless transmitter. Switch S_1 in

the converter was used to temporarily store energy in the inductor (L), and switch $S_2$was used to transfer the stored energy onto C_{DD} at the higher required voltage. Once C_{DD} had stored sufficient energy, the transmitter entered its active mode and wirelessly transmitted a packet to a nearby receiver, after which it returned to a low-leakage standby mode and the boost converter began to replenish C_{DD}. A start-up rectifier was used with an external wireless power source to initialize the system.

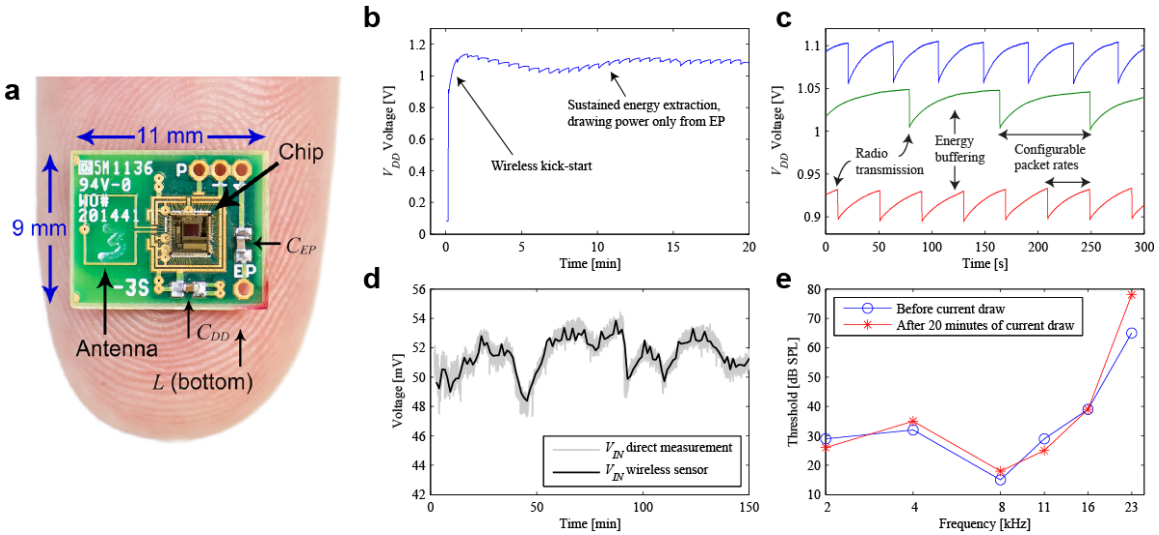

Figure 3 | Physical implementation and measurement results of the endoelectronics system. **a.** Photograph of the prototype endoelectronics board on a human index figure. **b.** Transient waveform of V_{DD} over the course of 20 minutes when operating with a guinea pig EP as the only source of energy into the system (apart from the initial wireless kick-start). **c.** Transient waveform of V_{DD} for three different experiments on three different animals. A 300 second time scale was used to show C_{DD} charging from the boost converter harvesting EP energy, as well as rapid periodic discharging from wireless transmissions. **d.** Measurement of V_{IN}, which is a measurement of EP following a voltage drop across the electrode impedance. The black line is measured by an external device

powered by a battery, while the light grey line is the V_{IN} estimate derived directly from the instantaneous data rate of wirelessly received data after a one-time normalization calibration. **e.** Compound action potential thresholds measured before and after the current extraction experiment shown in sub-panel **b**.

Online Methods:

Surgical procedures were performed at the Massachusetts Eye and Ear Infirmary with the approval of the institutional Animal Care Committee (protocol # 09-09-026). Animals were anesthetized and experiments were conducted in a heated, acoustically insulated chamber. Most animals had spontaneous, natural breathing. Mechanical ventilation was only used if respiration faltered due to anesthesia. The auricle and neighboring musculature were reflected ventrally to expose the external auditory meatus and bulla. The lateral wall of the bulla, up to the caudal edge of the tympanic ring, was removed to allow visualization of and access to the round window. Pulled glass microelectrodes, mounted on micromanipulators, were advanced through the round window to access the fluid spaces of the inner ear. The negative electrode was inserted into the perilymph-filled scala tympani, and the positive electrode was inserted through the basilar membrane and sensory epithelium into the endolymph-filled scala media (Supplementary Fig. 1). Microelectrodes were pulled from Borosil capillary tubing (FHC, Bowdoin, ME). The tips of electrodes were beveled at a 25^{o} angle using a BV-10 Microelectrode Beveler (Sutter Instruments, Novato, CA) to achieve tip diameters of ~2 μm and electrode impedance of ~400-800 kΩ for both electrodes. Electrodes were mounted in half-cell

holders containing Ag/AgCl exchange pellets (World Precision Instruments, Sarasota, FL). Electrolyte composition was 2 M KCl. All circuit grounds were with reference to perilymph.

Tone-pip audiograms were constructed by presenting brief tones (3.0 ms duration, 0.5 ms rise/fall times), at half-octave spacing between 2 - 32 kHz, to the external ear canal of the surgically targeted ear. The resulting compound-action potential was recorded using a metal-wire electrode placed adjacent to the round window. The threshold was defined as the minimum sound intensity required to elicit a response above 10 μV (the noise floor was measured to be approximately 4 μV).

The printed circuit board was manufactured with an FR-4 substrate, and the chip and two capacitors were mounted on the top of the board, while the inductor was mounted on the bottom. The chip was encapsulated by a non-conductive epoxy for mechanical stability (not shown in Fig. 3a for clarity). The system supply voltage was measured during *in vivo* experiments using a Keithley 2602 sourcemeter, while V_{IN} was measured using an Agilent U1253A set to 1GΩ input impedance. A wireless receiver, built using discrete components, was used to down-convert and record the instantaneous transmitter data rate on a Tektronix TDS3064B oscilloscope. The chip power consumption was measured during characterization experiments using a Keithley 6430 sourcemeter and high-isolation triaxial cables for accurate low-current measurements.

The chip was initialized with a wireless kick-start from an external RF source operating at 2.4 GHz placed several millimeters away for no more than two seconds. Due to on-chip voltage clamps, capacitor C_{DD}, which had a capacitance of 200 nF, charged to at

most 1.4 V during initialization. At 1.4 V, capacitor C_{DD} was storing E = $0.5C_{DD}V_{DD}^2$ = 200 nJ of energy. During operation, the boost converter, radio, and peripheral circuits consumed 573 pW (at 0.9 V). At this power consumption, the circuit would theoretically operate for at most 6 minutes before completely exhausting the energy stored on capacitor C_{DD}; in practice, time-to-exhaustion is typically much shorter. Taken together, any experiment lasting longer than a few minutes extracted energy from the EP.